

RNAi promotes heterochromatic silencing through replication-coupled release of RNA Pol II

Mikel Zaratiegui, Stephane Castel, Danielle Irvine, Anna Kloc, Jie Ren, Fei Li, Elisa de Castro, Laura Marín, An-Yun Chang, Derek Goto, et al.

► **To cite this version:**

Mikel Zaratiegui, Stephane Castel, Danielle Irvine, Anna Kloc, Jie Ren, et al.. RNAi promotes heterochromatic silencing through replication-coupled release of RNA Pol II. *Nature*, Nature Publishing Group, 2011, 479 (7371), pp.135-138. 10.1038/nature10501 . pasteur-02013927

HAL Id: pasteur-02013927

<https://hal-pasteur.archives-ouvertes.fr/pasteur-02013927>

Submitted on 13 Feb 2019

HAL is a multi-disciplinary open access archive for the deposit and dissemination of scientific research documents, whether they are published or not. The documents may come from teaching and research institutions in France or abroad, or from public or private research centers.

L'archive ouverte pluridisciplinaire **HAL**, est destinée au dépôt et à la diffusion de documents scientifiques de niveau recherche, publiés ou non, émanant des établissements d'enseignement et de recherche français ou étrangers, des laboratoires publics ou privés.

RNAi promotes heterochromatic silencing through replication-coupled release of RNA polIII

Mikel Zaratiegui (1), Stephane Castel (1,2), Danielle V. Irvine (1,6), Anna Kloc (1,6), Jie Ren (1), Fei Li(3,6), Elisa de Castro (4), Laura Marín (4), An-Yun Chang (1,5), Derek Goto(1,6), W. Zacheus Cande(3), Francisco Antequera (4), Benoit Arcangioli(1,7), Rob Martienssen(1,2)#

- (1) Cold Spring Harbor Laboratory, Cold Spring Harbor NY 11724
- (2) Watson School of Biological Sciences, Cold Spring Harbor Laboratory NY 11724
- (3) Molecular and Cellular Biology, University of California Berkeley
- (4) Instituto de Biología Funcional y Genómica. CSIC/Universidad de Salamanca. Spain
- (5) Molecular and Cellular Biology program, Stony Brook University, Stony Brook, New York 11794
- (6) Present address: Yale Stem Cell Center, Yale University, New Haven, CT (A.K.); Creative Research Initiative Sousei, Hokkaido University. Sapporo, Japan (D.G.); Department of Biology, New York University, New York, NY (F.L.); Murdoch Childrens Research Institute, University of Melbourne, Melbourne, Australia (D.V.I)
- (7) Permanent address: Institut Pasteur, Paris France.

#for correspondence, martiens@cshl.edu

Heterochromatin comprises tightly compacted repetitive regions of eukaryotic chromosomes. The inheritance of heterochromatin through mitosis requires RNA interference (RNAi), which guides histone modification¹ during the DNA replication phase of the cell cycle². Here, we show that the alternating arrangement of origins of replication and non-coding RNA in pericentromeric heterochromatin results in competition between transcription and replication. Co-transcriptional RNAi releases RNA polymerase II (PolII), allowing completion of DNA replication by the leading strand DNA polymerase, and associated histone modifying enzymes³ which spread heterochromatin with the replication fork. In the absence of RNAi, stalled forks are repaired by homologous recombination without histone modification.

In fission yeast, the Rik1/CLRC (Recombination in K, Cryptic Locus Regulator) complex silences heterochromatin via Clr4 and Lid2, which methylate histone H3 lysine 9 (H3K9) and demethylate histone H3 lysine 4 (H3K4), respectively². This complex is recruited in part by RNA interference, which processes non-coding transcripts found in the pericentromeric heterochromatin^{1,4}. Interactions between the RITS (RNAi transcriptional silencing) complex and CLRC have recently been found^{5,6}, but spreading of the Rik1 complex into reporter genes depends on the catalytic activity of RNAi, and the mechanism remains unknown⁷. Recently, we found that Cdc20 and Mms19 interact with Rik1 and are required for histone modification³. Cdc20 is the catalytic subunit of the leading strand DNA polymerase Pol Σ , while Mms19 is a regulatory subunit of the PolII transcription factor TFIIF. Both proteins participate in transcription coupled nucleotide excision repair (TC-NER) which depends on damage-stalled PolII to detect structural lesions in the DNA which are repaired by the Pol Σ after PolII release⁸.

The pericentromeric heterochromatin of fission yeast comprises outermost (*otr*) repeats called *dg* (5kb) and *dh* (1-6kb), flanked by innermost (*imr*) repeats (~6kb) containing clusters of tRNA genes (Fig. 1a). Histone H3 lysine-9 methylation is associated with *dg* and *dh* repeats (Fig. 1b), but ends abruptly at the tRNA clusters, and so is confined to heterochromatin⁹. The *dg* and *dh* repeats are transcribed by RNA polymerase II¹⁰, and processed into siRNA clusters up to 4.5kb in length (Fig. 1b). To investigate the extent of siRNA precursor transcripts, we first cloned and sequenced *dh* and *dg* repeat cDNA from *dcr1Δ* mutants (Fig. 1c). Polyadenylation sites were then identified using RACE-PCR (Methods), and sequencing revealed they were located within the clusters of siRNA (Fig. 1c). In previous studies of *dcr1Δ* mutants, PolII enrichment was detected by ChIP¹¹, while transcriptional run-on (TRO) analysis indicated over-accumulation of forward (but not reverse) transcripts¹. We found that these PolII ChIP (*cen-dg*) and TRO probes lie downstream of “forward” polyA sites (Fig. 1d), indicating inefficient termination and PolII readthrough in the absence of RNAi. To confirm readthrough, Northern blots of polyadenylated and total RNA from *dcr1Δ*, *ago1Δ* and *rdp1Δ* mutants were probed with strand specific probes. Transcripts corresponding to full length *dh* (1.3kb) and *dg* (1.3-2.3kb) cDNA clones were enriched in polyA+ RNA, as expected, but much longer readthrough transcripts up to 4.5kb could also be detected (Supplementary Fig. 1) indicating that polyadenylation was highly inefficient at these internal sites.

Inefficient polyadenylation is a strong indication of failure to release RNA polymerase II¹², and we hypothesized that slicing⁷ and dicing¹³ of nascent transcripts via RNAi promotes 3'-5' degradation by the exosome⁷ and release of RNA Polymerase II from the 3' end¹². The exosome is required for silencing consistent with this idea^{14 15}. To examine PolII release, we performed ChIP-seq with PolII antibodies, and found peaks of both poised (S5 phosphorylated)

and elongating forms (S2 phosphorylated) of PolIII in *dcr1Δ* mutants that corresponded to the polyadenylation sites on each strand (Fig. 1b,c). Peaks of siRNA accumulation mapped just downstream. Thus siRNA in WT cells accumulated where PolIII was released (Fig. 1b).

siRNA accumulate during S phase² and we found that siRNA clusters ended abruptly at the replication origin homology regions contained within each repeat¹⁶ (Fig. 1b). To assess the influence of DNA replication on PolIII accumulation we blocked replication in high concentrations of hydroxyurea (HU) and performed ChIP-seq using PolIII antibodies. In arrested *dcr1Δ* mutants, PolIII accumulated throughout the *otr* repeats, but in dividing *dcr1Δ* cells, PolIII accumulation was absent from replication origins (Fig. 2a and data not shown). To test if PolIII was expelled by replication fork progression (Fig. 2b), HU-arrested *dcr1Δ* cells were released into the cell cycle (Fig. 2c). As predicted, accumulation at replication origins was quickly lost, and PolIII was only found between origins, closer to promoters¹⁰, in each subsequent S phase.

Failure to release RNA polymerase II during S phase is a strong and robust signal for DNA damage⁸. In order to monitor DNA repair, the HU-arrested cells contained a Rad22-fusion protein Rad22-YFP. Rad22 (Rad52 in budding yeast) is essential for homologous recombination (HR) and is associated with single stranded DNA ends early during DNA repair. Chromatin immunoprecipitation revealed that Rad22^{Rad52} was weakly associated with heterochromatic origins in wild-type cells arrested with HU, but quickly declined following release (Fig. 2c). In *dcr1Δ* mutants, on the other hand, Rad22^{Rad52} peaked early in each successive S phase, indicating engagement of the repair machinery during heterochromatin replication¹⁷. In order to exclude the impact of HU arrest on DNA damage, we also examined Rad22-YFP accumulation in untreated WT and *dcr1Δ* mutant cells by fluorescence microscopy (Supplementary Fig. 2). The results were consistent with chromatin IP, in that 6 times as many *dcr1Δ* than WT cells had

Rad22^{Rad52} foci during septation (early S phase). Therefore, Dcr1 activity prevents DNA damage and the engagement of HR at the centromere.

We performed genetic tests to determine the role of RNAi in preventing DNA damage during S phase. DNA damage during replication can be rescued by HR repair, and we found that double mutants in the RecA homolog *rhp51^{rad51}* and *dcr1Δ* or *ago1Δ* were inviable or formed microcolonies (Fig. 2d). A similar requirement for Rhp51^{Rad51} has been demonstrated for convergent stalled replication forks¹⁸, which are protected from collapse in fission yeast by a stable replication-pausing complex comprising Swi1/Swi3 and Mrc1 (Mediator of replication checkpoint 1)¹⁹. Low concentrations of HU stalls replication forks, and we found that while *dcr1Δ*, *ago1Δ* and *rdp1Δ* cells were insensitive, double mutants with *swi3Δ* or *mrc1Δ* were very sensitive to low concentrations of HU (Supplementary Fig. 3). Similar results were obtained with Camptothecin (CPT) which causes arrest during S phase when the replication fork encounters the CPT-topoisomerase I complex. In genome-wide epistasis tests, mutants in more than 30 genes, mostly encoding proteins involved in DNA repair and histone modification interacted significantly with both *mrc1* and *dcr1*, forming a striking genetic network (Supplementary Table 1). This indicates that loss of Dcr1 activity engages replication fork protection.

In order to assess fork integrity, we examined replication of the repeats by 2D gel electrophoresis using probes from the *ura4* transgene, which was inserted into a passively replicated *dg* repeat on chromosome 1 (Fig. 2b). In WT cells, we detected strong X intermediates, indicative of joint molecules, as well as the expected fork or Y molecules (Fig. 3a). Similar X-DNA sister chromatid junctions arise at origins²⁰ but also at stalled replication forks²¹. These X-molecules were unaffected in *dcr1Δ* (Fig. 3b) but reduced in *mms19Δ*, in *swi6Δ* and especially in *clr4Δ* cells (Fig. 3c-e). Both Mms19 and Clr4 interact with Rik1, and Mms19

participates in transcription initiation³. Swi6 on the other hand is required to initiate replication within heterochromatic repeats¹⁷, and recruitment depends on Clr4. Thus simultaneous replication and transcription of heterochromatic repeats promote local replication fork stalling.

In WT cells (Fig. 4a), modified histones recruit Swi6 and the Rik1 complex via chromo- and other domains. Swi6 promotes early replication, and the Rik1 complex interacts with DNA Polε, which allows spreading of histone modification along with fork progression³. Flanking tRNA genes (Fig. 1a) pause replication²², preventing further spreading into neighboring euchromatin^{9,23}. Transcription during S phase stalls the replication fork, accounting for interactions between the replication and transcription machineries³, but RNAi releases PolII allowing replication to proceed. In the absence of RNAi (Fig. 4b), PolII remains stalled at replication forks and signals DNA repair by homologous recombination, which restarts blocked forks²⁴. The Rik1 complex is lost along with the replisome, preventing spreading of heterochromatin into reporter genes, which lose H3K9 methylation entirely. Recombination also removes modified histones from at least one of the two daughter chromatids²⁵ reducing, but not eliminating, methylation of the repeats as previously observed⁷.

We tested this model in several ways. First, we predicted that the interaction between the Rik1 complex and PolΣ should depend on RNAi, and we found that co-immunoprecipitation of Cdc20/ PolΣ with Dos2/Clr7 was reduced in *dcr1Δ* cells, along with H3K9me2 (Supplemental Fig. 4). Second, we observed that mutants in the cyclin-dependent PolII CTD kinase *cdk9* display slow growth and loss of pericentromeric silencing and sRNA (Supplemental Fig. 5). *cdk9* is a central regulator of transcription elongation that links cell-cycle regulated pre-mRNA

processing, co-transcriptional histone methylation and DNA damage²⁶. Finally, Clr4 has recently been found to have additional roles in recruiting the RNAi silencing RITS complex to accessory PolII factors²⁷, providing a potential mechanism for PolII release by RNAi. We found long transcripts indicative of strong transcriptional readthrough in *clr4Δ* mutant cells consistent with this model (Supplementary Fig. 1).

In the budding yeast *S. cerevisiae*, the Dicer-related RNase III Rnt1 releases PolII during transcription termination²⁸ while in *E. coli*, failure of transcription termination stalls replication forks and triggers recombination²⁹, providing a precedent for the mechanism we propose. According to this mechanism, transcription during S phase triggers histone modification, so long as RNA polymerase is released by RNAi, and not by homologous recombination repair. In plants, fungi and invertebrates, heterochromatic silencing may involve similar mechanisms (Supplemental Table 1), while in mammals, both X inactivation and imprinting require transcription of non-coding RNA in dividing cells³⁰. In each case, release of PolII during S phase, by RNAi or by other means, could allow fork restart and spreading of histone modification in a similar way.

Methods summary. Non-coding transcripts were cloned from a cDNA phage library by hybridization to *dh* and *dg* consensus probes. Cloning and high throughput sequencing of sRNA was performed using the Illumina genome analyzer according to manufacturer's instructions. Two dimensional gel electrophoresis of replication intermediates from steady state cultures was performed with probes to the *otr1::ura4+* insertion. For ChIP experiments, cultures were

arrested in 15mM HU for 4.5 hours, released and harvested at indicated times, to be crosslinked and processed for Chromatin immunoprecipitation.

References.

- 1 Volpe, T. A. *et al.* Regulation of heterochromatic silencing and histone H3 lysine-9 methylation by RNAi. *Science* **297**, 1833-1837 (2002).
- 2 Kloc, A., Zaratiegui, M., Nora, E. & Martienssen, R. RNA Interference Guides Histone Modification during the S Phase of Chromosomal Replication. *Curr Biol* **18**, 490-495 (2008).
- 3 Li, F., Martienssen, R. & Cande, W. Z. Coordination of DNA replication and histone modification by the Rik1-Dos2 complex. *Nature* **475**, 244-248 (2011).
- 4 Verdel, A. *et al.* RNAi-mediated targeting of heterochromatin by the RITS complex. *Science* **303**, 672-676 (2004).
- 5 Motamedi, M. R. *et al.* HP1 proteins form distinct complexes and mediate heterochromatic gene silencing by nonoverlapping mechanisms. *Mol Cell* **32**, 778-790 (2008).
- 6 Bayne, E. H. *et al.* Stc1: a critical link between RNAi and chromatin modification required for heterochromatin integrity. *Cell* **140**, 666-677, (2010).
- 7 Irvine, D. V. *et al.* Argonaute slicing is required for heterochromatic silencing and spreading. *Science* **313**, 1134-1137 (2006).
- 8 Svejstrup, J. Q. The interface between transcription and mechanisms maintaining genome integrity. *Trends Biochem Sci* **35**, 333-338 (2010).
- 9 Cam, H. P. *et al.* Comprehensive analysis of heterochromatin- and RNAi-mediated epigenetic control of the fission yeast genome. *Nat Genet* **37**, 809-819 (2005).
- 10 Djupedal, I. *et al.* RNA Pol II subunit Rpb7 promotes centromeric transcription and RNAi-directed chromatin silencing. *Genes Dev* **19**, 2301-2306 (2005).
- 11 Buhler, M., Verdel, A. & Moazed, D. Tethering RITS to a nascent transcript initiates RNAi- and heterochromatin-dependent gene silencing. *Cell* **125**, 873-886 (2006).
- 12 Rosonina, E., Kaneko, S. & Manley, J. L. Terminating the transcript: breaking up is hard to do. *Genes Dev* **20**, 1050-1056 (2006).
- 13 Djupedal, I. *et al.* Analysis of small RNA in fission yeast; centromeric siRNAs are potentially generated through a structured RNA. *EMBO J* **28**, 3832-3844 (2009).
- 14 Buhler, M., Haas, W., Gygi, S. P. & Moazed, D. RNAi-dependent and -independent RNA turnover mechanisms contribute to heterochromatic gene silencing. *Cell* **129**, 707-721 (2007).
- 15 Murakami, H. *et al.* Ribonuclease activity of Dis3 is required for mitotic progression and provides a possible link between heterochromatin and kinetochore function. *PLoS One* **2**, e317 (2007).
- 16 Smith, J. G. *et al.* Replication of centromere II of *Schizosaccharomyces pombe*. *Mol Cell Biol* **15**, 5165-5172 (1995).
- 17 Hayashi, M. T., Takahashi, T. S., Nakagawa, T., Nakayama, J. & Masukata, H. The heterochromatin protein Swi6/HP1 activates replication origins at the pericentromeric region and silent mating-type locus. *Nat Cell Biol* **11**, 357-362 (2009).

- 18 Lambert, S., Watson, A., Sheedy, D. M., Martin, B. & Carr, A. M. Gross chromosomal rearrangements and elevated recombination at an inducible site-specific replication fork barrier. *Cell* **121**, 689-702 (2005).
- 19 Shimmoto, M. *et al.* Interactions between Swi1-Swi3, Mrc1 and S phase kinase, Hsk1 may regulate cellular responses to stalled replication forks in fission yeast. *Genes Cells* **14**, 669-682 (2009).
- 20 Segurado, M., Gomez, M. & Antequera, F. Increased recombination intermediates and homologous integration hot spots at DNA replication origins. *Mol Cell* **10**, 907-916, (2002).
- 21 Minca, E. C. & Kowalski, D. Multiple Rad5 activities mediate sister chromatid recombination to bypass DNA damage at stalled replication forks. *Mol Cell* **38**, 649-661 (2010).
- 22 Deshpande, A. M. & Newlon, C. S. DNA replication fork pause sites dependent on transcription. *Science* **272**, 1030-1033 (1996).
- 23 Scott, K. C., Merrett, S. L. & Willard, H. F. A heterochromatin barrier partitions the fission yeast centromere into discrete chromatin domains. *Curr Biol* **16**, 119-129 (2006).
- 24 Lambert, S. *et al.* Homologous recombination restarts blocked replication forks at the expense of genome rearrangements by template exchange. *Mol Cell* **39**, 346-359 (2010).
- 25 Groth, A., Rocha, W., Verreault, A. & Almouzni, G. Chromatin challenges during DNA replication and repair. *Cell* **128**, 721-733 (2007).
- 26 Pirngruber, J., Shchebet, A. & Johnsen, S. A. Insights into the function of the human P-TEFb component CDK9 in the regulation of chromatin modifications and co-transcriptional mRNA processing. *Cell Cycle* **8**, 3636-3642 (2009).
- 27 Zhang, K. *et al.* Clr4/Suv39 and RNA quality control factors cooperate to trigger RNAi and suppress antisense RNA. *Science* **331**, 1624-1627, (2011).
- 28 Ghazal, G. *et al.* Yeast RNase III triggers polyadenylation-independent transcription termination. *Mol Cell* **36**, 99-109 (2009).
- 29 Washburn, R. S. & Gottesman, M. E. Transcription termination maintains chromosome integrity. *Proc Natl Acad Sci U S A* **108**, 792-797 (2011).
- 30 Pauler, F. M., Koerner, M. V. & Barlow, D. P. Silencing by imprinted noncoding RNAs: is transcription the answer? *Trends Genet* **23**, 284-292 (2007).

Supplementary Information is linked to the online version of the paper at

www.nature.com/nature.

Acknowledgements. We thank Donna Roh and Tom Volpe for isolating cDNA clones.

DI was supported by a NHMRC CJ Martin Postdoctoral Research Fellowship. MZ was

supported by a fellowship from the Spanish Ministry of Science. This work was supported by grants BFU2008-01919 and Consolider-Ingenio CSD2007-00015 from the Spanish Ministry of Science and Innovation to FA, and NIH R01 GM076396 to ZC and RM.

Author contributions. SC, DVI, AK, JR contributed equally to this work and are listed in alphabetical order. MZ, SC, DVI, AK, JR, FL, EdC, LM, AC and DG performed experiments, and SC analyzed the data. WZC, FA, BA and RM designed experiments and RM and MZ wrote the manuscript.

Author Information. Genomics data and analysis are available from the Gene Expression Omnibus (<http://www.ncbi.nlm.nih.gov/geo/>) accession number GSE30837. Individual cDNA sequences are available from GenBank (<http://www.ncbi.nlm.nih.gov/genbank/>) with accession numbers JN388396 to JN388565. Reprints and permissions information is available at www.nature.com/reprints. The authors declare no competing financial interests. Correspondence and requests for materials should be addressed to R.A.M. (martiens@cshl.edu).

Figure Legends.

Figure 1. Transcription and replication of pericentromeric heterochromatin in fission yeast.

a. Pericentromeric heterochromatin on Centromere 3. *dh* (red), *dg* (green) and *imr* (magenta) repeats are shown, bordered by tRNA genes (brown). Replication origins (yellow) are found in each repeat. **b.** Tiling microarrays of K9me2 ChIP (light blue) and clusters of small RNA sequences (dark blue) from wild-type cells. ChIP-seq reads corresponding to poised (S5-P) and elongating (S2-P) RNA polymerase II enriched in *dcr1Δ* cells relative to WT cells are in black. **c.** cDNA clones (beige) from *dcr1Δ* cells. PolyA sites are indicated as vertical lines and correspond to peaks of PolIII. Arrows indicate the direction of “Forward” transcription. **d.** Alignment of probes used in previous studies indicates that regions enriched for PolIII¹¹ (*cen-dg*) and transcriptional run-on probes¹ (TRO) lie downstream of forward orientation polyA sites

Figure 2. RNA interference and DNA replication restrict RNA polymerase II accumulation and prevent DNA damage.

a. Small RNA (blue) and PolIII ChIP-seq reads (black) from WT and *dcr1Δ* on the right arm of Centromere 1. **b.** A replication bubble is shown, initiated at one of the 3 origin homology regions at centromere 1 (yellow boxes). **c.** Chromatin immunoprecipitation for RNA PolIII and Rad22^{Rad52} from HU-arrested and released wild-type (dashed lines) and *dcr1Δ* (solid lines). Cell cycle progression after release from HU block is monitored by septation index, which peaks coincident with S phase. **d.** Representative parental and non-parental di-type tetrads from crosses between *rhp51Δ* cells, defective in homologous recombination, and *dcr1Δ* or *ago1Δ*.

Figure 3. Replication fork stalling during heterochromatin replication.

Replication intermediates in wild-type and mutant cells resolved by 2D gel electrophoresis and probed with the unique DS/E probe from the *ura4* transgene within the *dg* repeat on chromosome 1 (Fig. 2a). (a) A schematic of replication intermediates in 2D gels indicates joint molecules (X), and forks (Y). Junction molecules indicate fork stalling in (b) WT and (c) *dcr1Δ* mutant cells, and are reduced in (d) *mms19Δ*, (e) *swi6Δ* and (f) *clr4Δ*.

Figure 4. Replication-coupled transcriptional silencing through histone modification and RNAi.

a. The Rik1 complex (red octagon) is recruited to heterochromatic replication forks by interactions with methylated histone H3K9me2 and with the leading strand DNA polymerase (Pol Σ , green). Swi6 induces origin firing, but collision with RNA polymerase II (orange) stalls replication forks. RNAi releases PolIII by processing of pre-siRNA transcripts (red lines) allowing leading strand DNA polymerase to complete DNA replication and the associated Rik1 histone modification complex (red hexagon) to spread histone modification (black circles).

b. In the absence of RNAi, origins fire but PolIII is not released, stalling replication forks. Stalled PolIII signals repair via homologous recombination instead. Recombination could in principle occur with sister chromatids (shown here) or with other copies of the same repeat (not shown). DNA polymerase Σ and the associated Rik1 complex are lost along with the replisome, and fail to spread histone modification into neighboring reporter genes.

Supplementary Methods

Yeast strains and methods

S. pombe strains used in this study are listed in Table S2. Standard media and genetic protocols for fission yeast were used³¹. Crosses between *dcr1*, *ago1* and *rhp51* deletion mutant strains were performed with strains of h^+ , h^- and *smt-0* mating types, with comparable results. Lethality or sickness was observed in 90% of the double mutants as well as many single mutants, suggesting epigenetic effects inherited through meiosis.

cDNA analysis

Total RNA was extracted from cells growing in YES by the hot phenol method. In brief, mid-log phase (0.5 OD) yeast cultures were incubated in SDS-Acetate buffer (50 mM sodium acetate; 10 mM EDTA; 1% SDS pH 5), with an equal volume of Phenol pH 4.3 at 65°C for 15 minutes, vortexing every 2 minutes for 30 seconds. After centrifugation, the aqueous phase was extracted once with acid phenol, once with acid Phenol:Chloroform 1:1 and precipitated by addition of 1/10 volume of 3M sodium acetate pH 8 and 2 volumes of ethanol, resuspended and treated with the DNafree kit (Ambion). cDNA was reverse transcribed from total RNA using oligodT adapters, and cloned into phage vectors as recommended by the supplier (Stratagene). More than 60 clones were purified by blot hybridization to *dg* and *dh* probes, and sequenced from both ends. Polyadenylation sites were identified by a string of T residues longer than the adaptor followed by matches to the *S. pombe* consensus sequence. Alignment to the genome sequence was possible because of single nucleotide polymorphisms between copies of the repeats, with the exception of chromosome 3, where the tandemly arranged *dg* and *dh* repeats are identical. Sequences containing a long stretch of A residues immediately downstream of known centromeric sequence were considered to represent the polyadenylated 3' ends of centromeric transcripts. Polyadenylation sites of centromeric cDNA sequences from WT and $\Delta rdr1$ strains were determined using the LM-PAT assay as previously described³² with the following message specific primers: dgIIIrevPolC, dgIIIrevPolD, dgIIIforPolC, dhIforPolA and dhIrevPolA. The PCR products amplified from LM-PAT cDNA were separated on an agarose gel, individually extracted and cloned into the pCR2.1-TOPO vector (Invitrogen) according to the manufacturers instructions. Cloned products were then sequenced in both directions. See oligo list for details (Supplementary Table S3).

Northern blot analysis

Total RNA was extracted from cells growing in YES by the hot phenol method. PolyA⁺ RNA was isolated from WT and mutant strains using Dynabeads Oligo(dT) (Invitrogen). Northern blot analysis was performed using NorthernMax-Gly (Ambion). Blots were probed for the *dh* transcripts (p30_F_T7 and p30_R_T3), *dg* transcripts (p33_F_T7 and p33_R_T3) and actin (act1F and act1R_T7). See oligo list (Supplementary Table S3) for details.

Small RNA library sequencing

Total RNA was extracted from cells growing at exponential phase in YES using hot phenol extraction. Small RNAs were isolated using Flashpage followed gel isolation. Small RNA libraries for Solexa/Illumina sequencing were prepared according to the manufactures instructions. Libraries were sequenced on an Illumina Genome Analyzer. The resulting sequence

reads, including quality scores, were aligned to the *S. pombe* reference sequence using MAQ (<http://maq.sourceforge.net/>) using the ‘map’ function.

Two-dimensional gel electrophoresis

Two-dimensional gel electrophoresis of centromeric DNA was performed as previously described⁵. DNA pellets were digested with NcoI/HindIII to generate restriction fragments of 3.7 kb for origin 2055 and 4.0 kb for the *otr::ura4⁺* transgene at the centromere. The two restriction fragments were analyzed using probe to 2055²⁰ and a probe that recognizes the *ura4-DS/E* minigene deleted region. See oligo list for details (Supplementary Table S3).

Hydroxyurea Synchronization and Chromatin Immunoprecipitation

Synchronization of log phase *rad22-yfp* and *rad22-yfp/Δdcr1 S. pombe* strains was performed as previously described². In brief, cells were treated with 15mM hydroxyurea (HU) (Sigma) for 4.5 hr to synchronize in S phase. Cells were released by washing twice in HU free media and grown for 5 hrs taking 50 ml samples every 30 minutes. Samples were fixed with 3% paraformaldehyde for chromatin immunoprecipitation (ChIP) as previously described⁷. Chromatin was purified, sonicated and incubated with either anti-RNA Polymerase II (clone 8WG16, Upstate) or anti-GFP (Roche) antibodies. Synchronization efficiency was estimated using the septation index. For ChIP quantification, immunoprecipitated DNA was amplified by quantitative PCR (qPCR) in duplicate. The following formula was used: enrichment = $2^{-((C_{idh-Ciact1})_{IP} - (C_{idh-Ciact1})_{wce})}$. The test regions were amplified with the following primers; p30F_qPCR and p30R_qPCR (*dh* region), p33F-qPCR and p33R_qPCR (*dg* region), and p20F and p20R (2055 origin of replication), and for the reference, act1F_qPCR and act1R_qPCR (*act1*). See oligo list for details (Supplementary Table S3).

Chromatin Immunoprecipitation sequencing and data analysis

Samples from log phase DG21 and DG690 *S. pombe* strains were fixed (dividing cells) or first treated with 15mM hydroxyurea (HU) (Sigma) for 4.5 hr, washed once in HU free media and fixed (HU arrested cells)². Chromatin was purified, sonicated and incubated with following anti-RNA Polymerase II antibodies from Abcam: clone pospho-S2 (ab5095), and clone pospho-S5 (ab5131). For ChIP-seq, immunoprecipitated DNA was polished, ligated and amplified with the Illumina ChIP-seq sample preparation kit according to the manufacturer’s instructions, and sequenced in an Illumina Hi-Seq 2000 analyzer by 50bp paired end sequencing as previously described³³. Analysis was carried out by a custom pipeline using Bowtie to align reads to the *S. pombe* genome and MACS 1.4 for significance enrichment calls³⁴. Wiggle fragment pileup files were generated for each comparison to visualize the difference in PolIII enrichment between control (DG21) and treatment (DG690) IPs at 10bp intervals genome wide. The difference at each interval was calculated by first normalizing to the total number of reads between the two by scaling up, and then subtracting the normalized control value from the treatment. Detailed sequence statistics are provided in Table S4.

Microscopy

Samples were analyzed using differential interference contrast (DIC) microscopy and fluorescence microscopy (Axioimager Upright Fluorescent Microscope).

Survival assays

Midlog phase cultures were resuspended to 2×10^6 cells/ml and serially diluted tenfold. Dilutions were spotted on YES agar plates or YES agar containing the indicated amounts of hydroxyurea (HU) (Sigma), camptothecin (CPT) (Sigma), or methyl methanesulfonate (MMS) (Sigma). Recovery was for 3 days at 30°C.

Co-Immunoprecipitation

Cells were lysed by glass beads in HB buffer³¹. Lysates were pre-cleared with protein A agarose beads, followed by 2-hour incubation with antibodies against HA tag (Sigma, E6779) at 4°C. After washing, eluted proteins and input extracts were analyzed by Western blotting using antibodies against TAP (Sigma, P 2026).

Additional references for methods.

- 31 Moreno, S., Klar, A. & Nurse, P. Molecular genetic analysis of fission yeast *Schizosaccharomyces pombe*. *Methods Enzymol* 194, 795-823 (1991).
- 32 Sallés, F.J., Richards, W.G., Strickland, S. Assaying the Polyadenylation State of mRNAs. *Methods* 17, 38-45.
- 33 Zaratiegui M., Vaughn M.W., Irvine D.V., Goto D., Watt S., Bähler J., Arcangioli B., Martienssen R.A. CENP-B preserves genome integrity at replication forks paused by retrotransposon LTR. *Nature* 469, 112-115, (2011).
- 34 Zhang Y., Liu T., Meyer C.A., Eeckhoutte J., Johnson D.S., Bernstein B.E., Nusbaum C., Myers R.M., Brown M., Li W., Liu X.S. Model-based analysis of ChIP-Seq (MACS). *Genome Biol* 9, R137, (2008).

Figure 1:

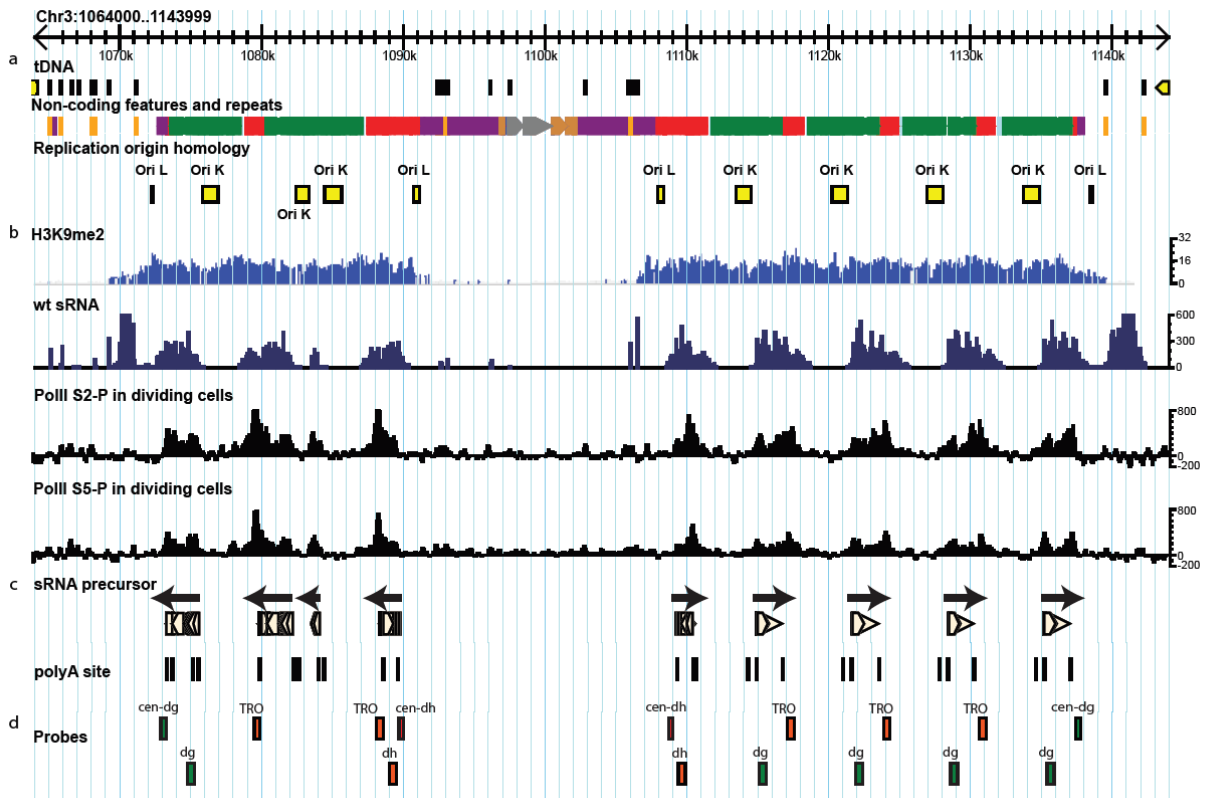
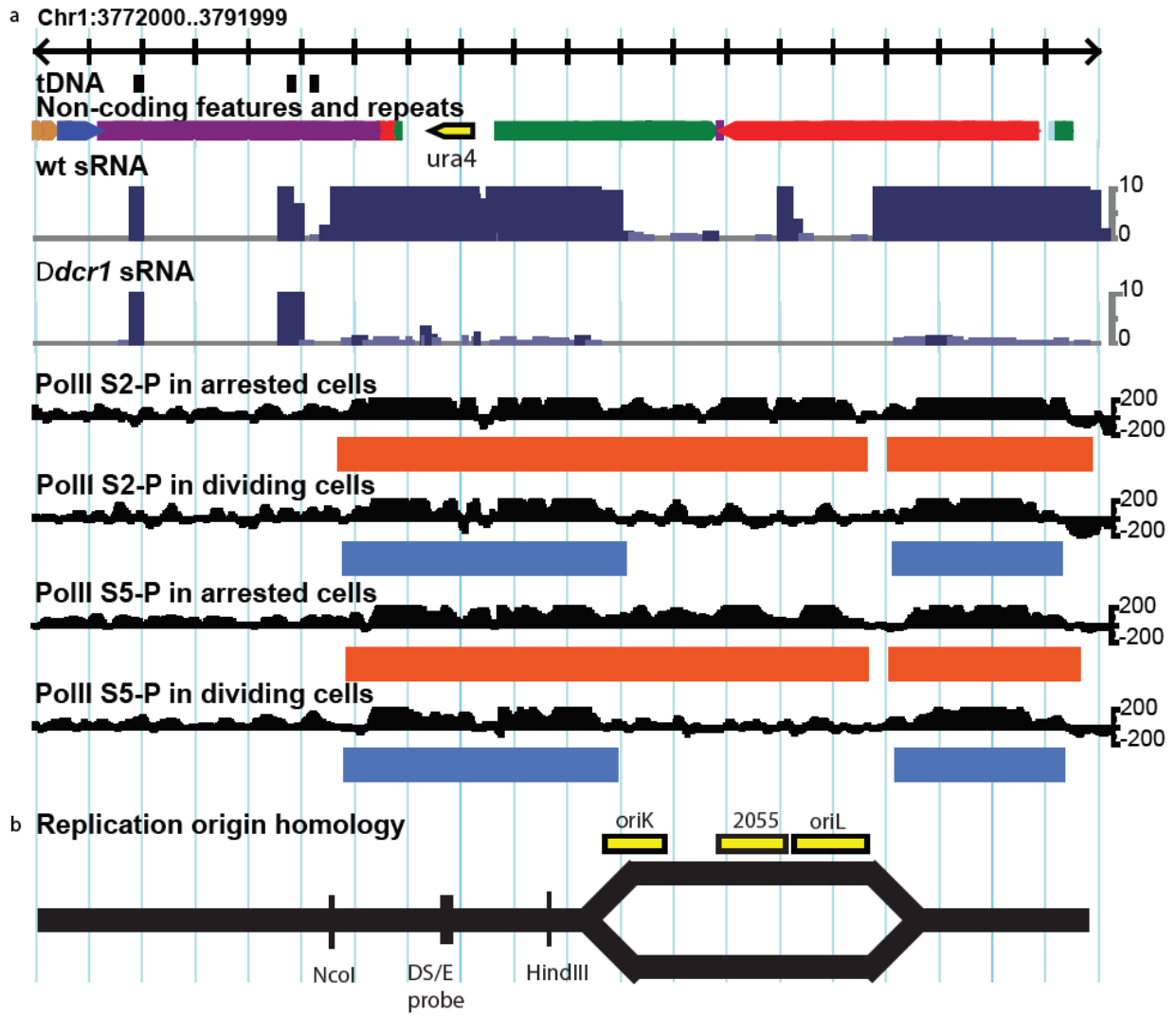
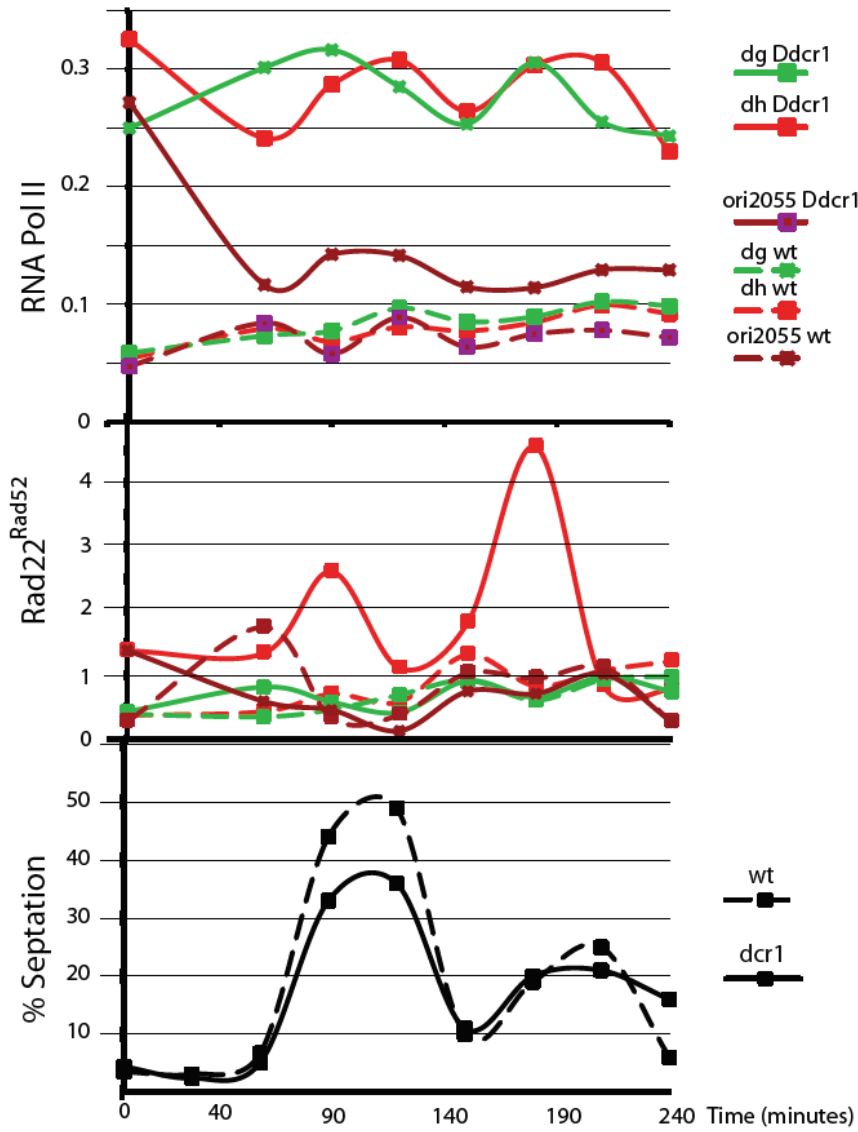


Figure 2:

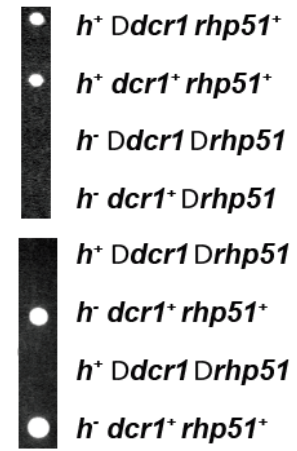


c



d

Ddcr1 x Drhp51



Dago1 x Drhp51

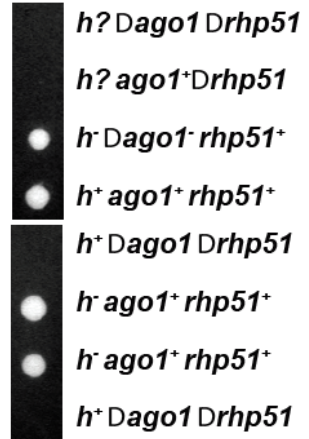


Figure 3 :

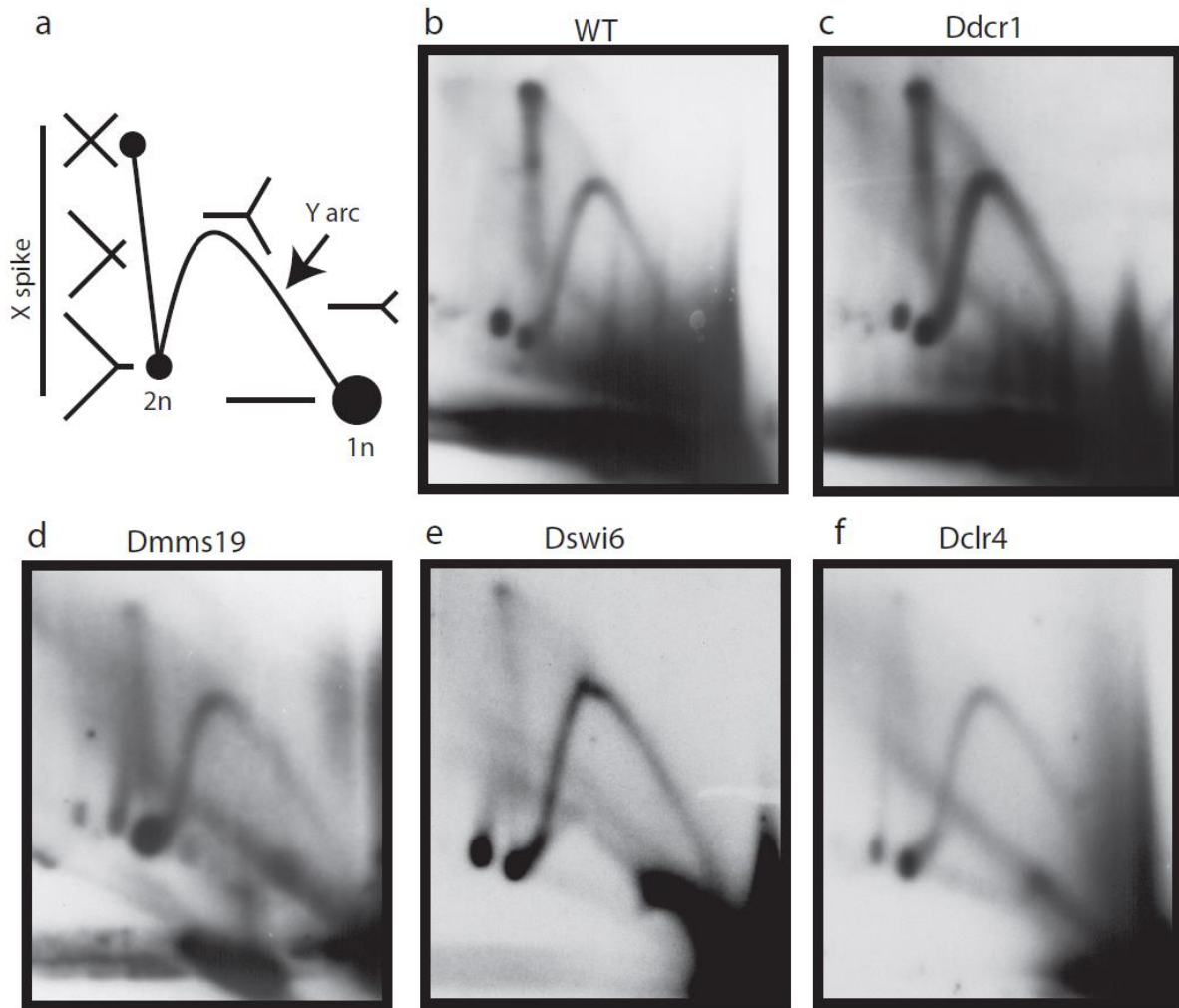


Figure 4 :

